

Using gold nanoparticles for enhanced intradermal delivery of poorly soluble auto-antigenic peptides

R K Singh, C. Malosse, J. Davies, Bernard Malissen, E. Kochba, Y. Levin, J C Birchall, S A Coulman, J Mous, M A Mcateer

▶ **To cite this version:**

R K Singh, C. Malosse, J. Davies, Bernard Malissen, E. Kochba, et al.. Using gold nanoparticles for enhanced intradermal delivery of poorly soluble auto-antigenic peptides. Nanomedicine: Nanotechnology, Biology and Medicine, 2020, 10.1016/j.nano.2020.102321 . hal-03013467

HAL Id: hal-03013467
https://hal.science/hal-03013467

Submitted on 23 Nov 2020

HAL is a multi-disciplinary open access archive for the deposit and dissemination of scientific research documents, whether they are published or not. The documents may come from teaching and research institutions in France or abroad, or from public or private research centers.

L'archive ouverte pluridisciplinaire **HAL**, est destinée au dépôt et à la diffusion de documents scientifiques de niveau recherche, publiés ou non, émanant des établissements d'enseignement et de recherche français ou étrangers, des laboratoires publics ou privés.

Nanomedicine: Nanotechnology, Biology, and Medicine
xx (xxxx) xxx

nanomedicine
Nanotechnology, Biology, and Medicine

nanomedjournal.com

Using gold nanoparticles for enhanced intradermal delivery of poorly soluble auto-antigenic peptides☆,☆☆,☆☆☆

R.K Singh[a,1], C. Malosse[b], J. Davies[a], B. Malissen[b,c], E. Kochba[d], Y. Levin[d], J.C Birchall[e], S.A Coulman[e], J. Mous[f,2], M.A McAteer[f], C.M Dayan[a,*], S. Henri[b], F.S Wong[a]

[a]*Division of Infection & Immunity, School of Medicine, Cardiff University, Heath Park, Cardiff, UK*
[b]*Centre d'Immunologie de Marseille-Luminy, Aix Marseille Université, Inserm, CNRS, Marseille, France*
[c]*Centre d'Immunophénomique, Aix Marseille Université, INSERM, CNRS, Marseille, France*
[d]*NanoPass Technologies Ltd., Nes Ziona, Israel*
[e]*School of Pharmacy and Pharmaceutical Sciences, Cardiff University, UK*
[f]*Midatech Pharma PLC, Cardiff, UK*

Revised 8 August 2020

Abstract

Ultra-small 1-2 nm gold nanoparticles (NP) were conjugated with a poorly-soluble peptide auto-antigen, associated with type 1 diabetes, to modify the peptide pharmacokinetics, following its intradermal delivery. Peptide distribution was characterized, in vivo, after delivery using either conventional intradermal injection or a hollow microneedle device. The poorly-soluble peptide was effectively presented in distant lymph nodes (LN), spleen and draining LN when conjugated to the nanoparticles, whereas peptide alone was only presented in the draining LN. By contrast, nanoparticle conjugation to a highly-soluble peptide did not enhance in vivo distribution. Transfer of both free peptide and peptide-NPs from the skin to LN was reduced in mice lacking lymphoid homing receptor CCR7, suggesting that both are actively transported by migrating dendritic cells to LN. Collectively, these data demonstrate that intradermally administered ultra-small gold nanoparticles can widen the distribution of poorly-soluble auto-antigenic peptides to multiple lymphoid organs, thus enhancing their use as potential therapeutics.
© 2020 Published by Elsevier Inc.

Key words: Gold nanoparticles; Hydrophobic; Peptide; Intradermal; Microneedle; Autoantigen

Type 1 diabetes is an autoimmune disease characterized by the destruction of insulin-producing beta cells within the pancreas.[1] Insulin maintains blood glucose levels but is not a cure. Hence, we seek strategies to deliver antigen-specific immunotherapy to reduce immune-mediated beta cell damage.

The skin is an accessible route for therapeutic delivery. The rich network of antigen-presenting cells, including epidermal Langerhans and dermal dendritic cells (DCs) in skin, facilitates both immune activation and regulation, upon delivery of a therapeutic.[2–5] Microneedles (MNs) are a viable alternative to conventional hypodermic needles for intradermal (ID) delivery, being both minimally invasive and relatively pain-free.[6,7] A variety of MNs exists, including the 600 μm hollow MNs (MicronJet600™), which have been used in this study and in the clinical setting to deliver insulin,[8] influenza vaccine,[9,10] zoster vaccine[11] and polio.[12,13] MicronJet600™ hollow MNs reproducibly and effectively deliver material into the dermal compartment, with a significant vaccine dose-sparing effect and improved immunogenicity, compared with intramuscular and subcutaneous delivery.[14]

☆ **Funding:** This work was part of the EE-ASI European research network (Collaborative Project) supported by the European Commission under the Health Cooperation Work Programme of the 7th Framework Programme (grant agreement no. 305305).
☆☆ **Conflicts of interest:** none
☆☆☆ **Prior presentation:** Some of this work was presented in abstract form at the Immunology of Diabetes Society meetings in Munich in 2015 and San Francisco in 2017

*Corresponding author at: Division of Infection & Immunity, School of Medicine, Cardiff University, Heath Park, Cardiff, UK.
E-mail address: dayancm@cardiff.ac.uk. (C.M. Dayan).
[1] **Present address Department of Oncology, University of Oxford, Oxford, UK
[2] Present address MRM Consulting GmbH, Switzerland.

https://doi.org/10.1016/j.nano.2020.102321
1549-9634/© 2020 Published by Elsevier Inc.

UNCORRECTED PROOF

Nanoparticles (NPs) can be conjugated to multiple therapeutics, including peptides, as drug delivery agents. They can protect peptides from degradation, and can form a depot at the site of injection so enhancing antigen retention and uptake by DCs. Moreover, small carbohydrate-coated gold NPs also offer reduced toxicity[15] and bio-compatibility as well as exhibiting anti-inflammatory properties.[16] Furthermore, gold (Au) can be easily and covalently decorated on its surface by exploiting the strong soft–soft interaction between Au atoms and sulfur. Therefore, gold NPs represent a versatile nanoplatform for development of epitope-based vaccines.[17]

Recently, NPs have been used to prevent autoimmune diabetes in the non-obese diabetic (NOD) mouse model of diabetes by generating tolerogenic DCs and promoting T regulatory cell expansion to re-establish immune tolerance.[18,19] Although promising, both studies utilized systemic (intravenous or intraperitoneal) delivery systems, as well as large (>50 nm) NPs. In humans, skin-mediated delivery is more practical and convenient, has fewer safety concerns and can exploit the local immune cells. We have recently demonstrated that gold NPs (Midacore™) (<5 nm hydrodynamic radius), conjugated to a peptide autoantigen, can be effectively delivered into the dermal and epidermal layers of human skin explants by MicronJet600™ hollow MNs and target local antigen-presenting cells.[20] This present study is the first published report exploring the in vivo pharmacokinetics and resulting systemic immune response following MN-mediated delivery of a poorly-soluble autoantigenic peptide conjugated to ultra-small gold NPs.

Methods

Animal models

BDC2.5 TCR transgenic NOD mice[21] have diabetogenic CD4+ T-cells that recognize a hybrid insulin-chromogranin A peptide (HIP)[22] and mimotope peptides (the specific one used in this study is designated BDC2.5mimotope peptide).[23] The mice were purchased from the Jackson laboratory and have been bred in a specific pathogen-free facility of Cardiff University. OTII TCR transgenic C57BL/6J mice[24] and CCR7$^{-/-}$mice[25] on the C57BL/6J genetic background have previously been described. C57BL/6J mice were purchased from Janvier (France). Mice were maintained in individually-ventilated filter cages in scantainers on a 12 h light/dark cycle. Animal procedures were approved by University ethical review committee. All procedures relating to NOD mice were performed in accordance with protocols approved by the UK Home Office. All procedures relating to OTII and CCR7$^{-/-}$ mice were carried out in accordance with French and European directives.

Peptides and solubility

The peptides (physiochemical properties shown in Table 1) were purchased from Peptide Synthetics, manufactured to >95% purity: BDC2.5mimotope – YVRPLWVRME; Hybrid Insulin Peptide (HIP) – DLQTLALWSRMD; Ovalbumin323-339 peptide (OTII)-ISQAVHAAHAEINEAGR.

NP synthesis/characterization

Gold NPs (Midacore™) with a gold core size of <5 nm were synthesized and supplied by Midatech Pharma.[20] NPs were conjugated with each of the poorly-soluble HIP and BDC2.5mimotope peptides as well as the highly-soluble ovalbumin peptide, OTII, using custom-synthesized peptides with a thiol propionic acid linker, in an amide linkage at the N terminal (–S(CH2)2– CONH) (AmbioPharm Inc., North Augusta, SC, USA). Figure 1 illustrates the schematic structure of NPs covalently linked to BDC2.5mimotope peptide and Table 2 summarizes the NP properties. For all reactions, gold (III) chloride was mixed with a 3-fold excess of organic ligands and peptide in different ratios (5% β glucose C2 (synthesized in-house) and either 94% or 92% L-glutathione oxidized (Sigma Aldrich) and 1% or 3% peptide). Glutathione enabled non-enzymatic intracellular activation and release. The NPs were produced by reduction, following rapid addition of a 20-fold molar excess, relative to gold, of freshly-made 1 M sodium borohydride (Sigma Aldrich, Poole, UK) under vigorous vortex mixing. The samples were continuously vortexed for 1 min followed by a further 1 h constant mixing on a flatbed shaker at room temperature. After 1 h, the NP samples were concentrated by ultrafiltration using Amicon Ultra-15 centrifugal filter tubes (Millipore Ltd., 10 K membrane molecular weight cut-off) and washed 4 times with Milli-Q water (4 ml) to remove unbound peptide and residual borohydride.

The NP gold content was determined using a colorimetric gold assay. Hydrodynamic size and zeta potential of the NPs in water/10% PBS were determined by dynamic light scattering (DLS) using a Zetasizer Nano ZSP (Malvern instruments). Peptide content of the NP samples was determined by HPLC using a Varian 900-LC, with a reverse phase C18 column (Acquisition time: 11.2 min; Temperature = 35 °C; Slit width = 2 nm; 95% water, 5% acetonitrile gradient (1 ml/min) switching at 8 min, switch to 20% water, 80% acetonitrile). In brief, an aliquot of NPs (10 μl) was mixed with 40 μl of KCN solution (100 mM in 10 mM potassium hydroxide) to dissolve the gold. The sample was analyzed by HPLC at 212 nm to determine released peptide concentration, and at 400 nm to confirm that all the gold was dissolved. An aliquot of NPs (10 μl), diluted with 20 μl TFA, was also analyzed by HPLC to determine whether any free peptide remained in the NP solution, following ultrafiltration purification.

ID injection of peptide-loaded NPs

Mice were anesthetized using isoflurane and the injection site was shaved prior to delivery. Free peptide or peptide-loaded NPs were injected intradermally in 50 μl sterile PBS using a 29G needle.

MN characterization and injection of peptide-loaded NPs

Hollow MN devices (MicronJet600™) were provided by NanoPass Technologies. MicronJet is a CE marked and FDA cleared device, consisting of three MNs, each 600 μm in length, with a lumen of approximately 60 μm in diameter, bonded to a plastic adapter that attaches to a Luer syringe.[14] MicronJet600 ™

UNCORRECTED PROOF

ARTICLE IN PRESS

t1.1 Table 1
t1.2 Physicochemical properties of peptides used, listed in order of hydrophobicity with BDC2.5 being the most hydrophobic and OVA being the least hydrophobic (genscript online resource, available at https://www.genscript.com/ssl-bin/site2/peptidecalculation.cgi).

t1.3 Peptide	Sequence	Charge	Isoelectric point	pH	% hydrophobic/hydrophilic residues
t1.4 BDC2.5	YVRPLWVRME	1	9.34	Basic	Hydrophobic: 60% Hydrophilic: 10% Neutral: 30%
t1.5 HIP	DLQTLALWSRMD	−1	4.11	Acidic	Hydrophobic: 50% Hydrophilic: 25% Neutral: 25%
t1.6 OTII	ISQAVHAAHAEINEAGR	1	6.5	Basic	Hydrophobic: 47.1% Hydrophilic: 23.5% Neutral: 29.4%

injection did not change the diameter of NPs, which remained physically stable under the shear forces of the injection.[26] Mice were anesthetized using isoflurane, the injection site was shaved, and peptide was injected in 50 μl sterile PBS.

Adoptive cell transfer

Splenic BDC2.5 CD4+ T-cells were purified using a MACS CD4 II negative selection kit (Miltenyi Biotec). Cells were labeled with 20 μM CFDA (Invitrogen) in 10% fetal calf serum (FCS) RPMI at room temperature for 5 min at a concentration of 10^7/ml. The cells were then washed twice in RPMI containing FCS, rested for 15 min, and subsequently washed in saline. These cells were then re-suspended at 4×10^6 cells in 200 μl sterile saline and injected intravenously into 6-10-week-old female mice. At the indicated times, single-cell suspensions were prepared from spleen and various LNs, and $CD4^+$ T-cells were analyzed by FACS. OTII T-cells were isolated from pooled LNs and spleen of OTII mice, maintained on a *Rag-2*$^{-/-}$xB6 [CD45.1] background, using a $CD4^+$ T-cell negative isolation kit (Dynal, Invitrogen). For CTV labeling, purified OTII T-cells were resuspended in PBS containing 2.5 mM cell tracer violet (CTV) (Molecular Probes) for 3 min at room temperature. 10^6 CTV-labeled OTII T-cells were adoptively transferred into the specified mice.

Phenotypic analysis by flow cytometry

All antibodies were purchased from BioLegend and BD Pharmingen.

A single cell suspension was pre-treated with anti-CD16/32 (BD Pharmingen) and then stained at 4 °C for 25min with the following pre-titrated mAbs against the indicated antigens: CD4-AF700 (RM4-5), CD44-BV71 (IM7), CD3e-AF700 (500A2), CD45.1-APC (A20), CD4-BV786 (RM4-5) and TCR Vα2-PE (B20.1). To assess intracellular expression, samples were permeabilized and fixed using Foxp3 transcription factor staining buffer set (eBioscience), according to the manufacturer's instructions. Intracellular mAbs against the following proteins included: CTLA4-BV421 (UC10-4B9), IL10-BV650 (JES5-16E3) and IFNγ-PeCY7 (XMG-1.2). Cell viability was evaluated using fixable viability dye efluor780 (eBioscience) or zombie yellow (Biolegend), according to the manufacturer's instructions. Samples were washed and read using a FACS LSRII Fortessa cytometer with DIVA software (BD) and analyzed using FlowJo software (Treestar).

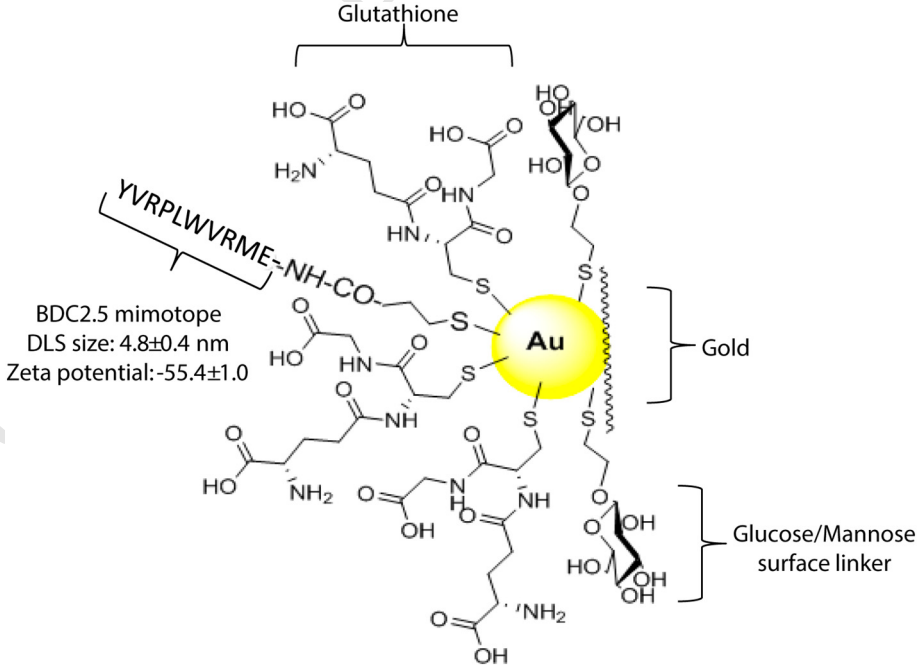


Figure 1. **Gold NP composition**. Composition of gold NPs used, comprising a gold core, conjugated via sulfur bonds to an organic layer of glucose or mannose, glutathione and peptide, (BDC2.5mimotope).

t2.1 Table 2
t2.2 NP properties, including DLS size, NP zeta potential and peptide loading levels.

t2.3 Peptide	DLS size (nm)	Zeta potential	Peptide loading levels
t2.4 BDC2.5	4.8 ± 0.4	−55.4 ± 1.0	2%
t2.5 HIP	3.3 ± 1.0	−54.7 ± 1.0	2%
t2.6 OVA	6.3 ± 0.8	−45.3 ± 0.6	2%

Statistical analysis

All results are presented as the mean ± standard error of the mean (SEM) and were analyzed using GraphPad Prism V5. Student's *t* test, one-way ANOVA and two-way ANOVAs (for analyses with more than 1 variable) with Bonferroni post-hoc test were used for statistical analysis. P values of <0.05 were considered statistically significant: *denotes $P < 0.05$, **denotes $P < 0.01$, ***denotes $P < 0.001$.

Results

Pharmacokinetics of intradermally-delivered BDC2.5mimotope peptide coupled to NP differs from BDC2.5mimotope peptide alone in vivo

Following the intravenous transfer of CFDA-labeled islet-specific BDC2.5 CD4+ T-cells into naïve NOD mice, BDC2.5mimotope NPs, BDC2.5mimotope peptide alone (2 μg peptide in 50 μl) or peptide free 'blank' NPs were administered by ID injection at the back of the neck. Lymphoid organs were then analyzed at 24, 48 and 72 h. Following administration of BDC2.5mimotope NPs, BDC2.5 T-cell proliferation in the skin-draining LN (axillary), the non-draining LN (inguinal), the spleen and pancreatic LN (PLN) was enhanced, compared to baseline at the 48 and 72 h time points (Figure 2). In contrast, levels of proliferation were much reduced in mice treated with BDC2.5mimotope peptide alone; proliferation was only detected in the axillary (draining) LN at the 72 h time point, with no proliferation at either 24 or 48 h (and only baseline proliferation in the PLN) (Figure 2). As expected, modest proliferation of BDC2.5 CD4+ T-cells as a result of endogenous presentation of the cognate antigen occurred in the pancreatic LN in control mice. This was not enhanced following ID injection of peptide and indicates that the peptide administered alone was not disseminated to the PLN. No proliferation was observed using peptide-free 'blank' NPs, confirming the antigen-specific nature of the response. Overall, ID delivery of BDC2.5mimotope peptide via NPs resulted in significantly higher levels of T-cell proliferation in distant lymphoid tissues and at earlier time points than peptide alone.

Peptide NP conjugation: the effects of T-cell affinity

CD4+ T-cells are central in the process of beta cell destruction. BDC2.5 CD4+ T-cells are highly diabetogenic and

PROOF

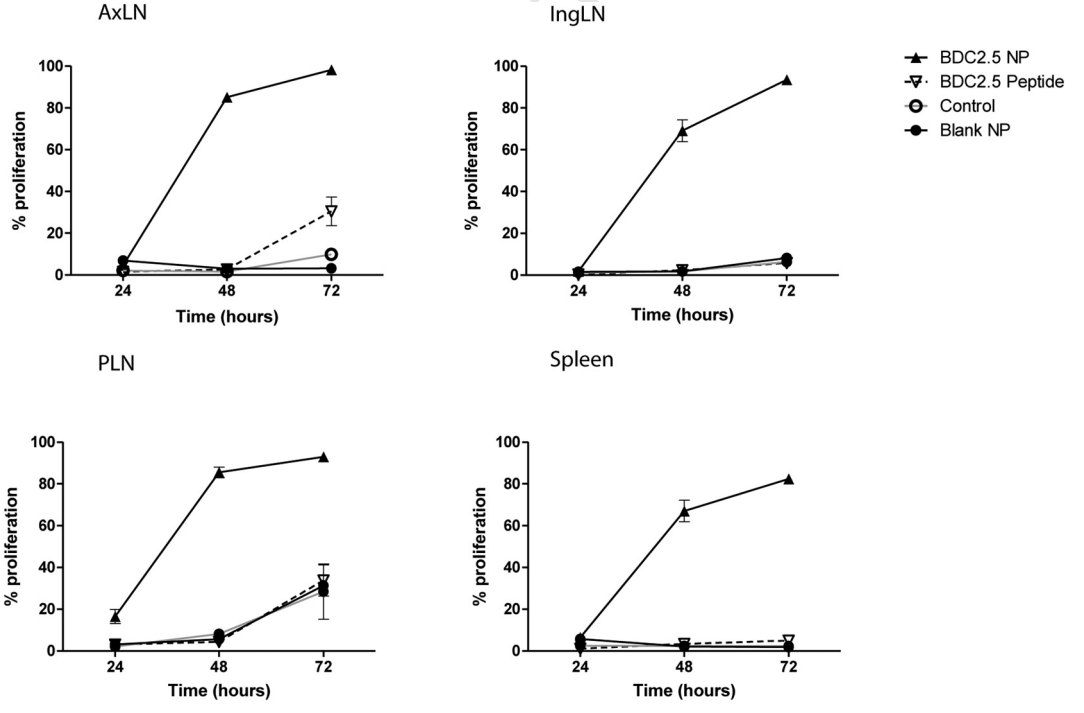


Figure 2. **In vivo proliferation time course analysis following peptide-NP delivery compared to peptide alone.** CFDA-labeled BDC2.5 CD4+ T-cells were transferred intravenously into NOD mice, followed by an ID injection of either 2 μg BDC2.5mimotope or BDC2.5mimotope-NP or peptide free 'blank' NP. Experimental control mice did not receive the ID injection. LNs (axillary, inguinal and pancreatic) and spleen were harvested at 24, 48 and 72 h following injection and BDC2.5 CD4+ T-cells analyzed for proliferation by CFSE dilution. Mean ± SEM with 3 mice per treatment is shown, representative of 3 experiments. Statistical analysis was done by two-way ANOVA with Bonferroni post-test comparing BDC2.5mimotope NP to BDC2.5mimotope peptide (***$P < 0.001$).

the natural epitope for these pathogenic cells is a hybrid insulin peptide (HIP), formed by the fusion of a chromogranin A peptide sequence WE14 and insulin C-peptide.[22] Although naturally formed, HIP has a lower affinity for BDC2.5 CD4+ T-cells than the commonly used high affinity islet antigenic peptide substitute BDC2.5mimotope. Therefore, to determine whether NP conjugation changed these relative peptide affinities, NPs were conjugated to either the high affinity BDC2.5mimotope peptide or the lower affinity naturally-formed HIP peptide. CFDA-labeled BDC2.5 CD4+ T-cells were then intravenously transferred into NOD mice and these mice were subsequently treated with an ID injection of an NP formulation (BDC2.5mimotope or HIP peptide or peptide alone. At 72 h, proliferation of transferred BDC2.5 CD4 T-cells was significantly higher in all lymphoid tissues following treatment with the BDC2.5 NPs compared to BDC2.5mimotope peptide (Figure 3, *A* and *B*), replicating earlier findings shown in Figure 2. However, this effect was not observed using the lower affinity HIP-NPs at an equivalent peptide dose (2 μg). Instead, HIP-NPs only induced proliferation in the axillary LN and at lower levels than those seen with

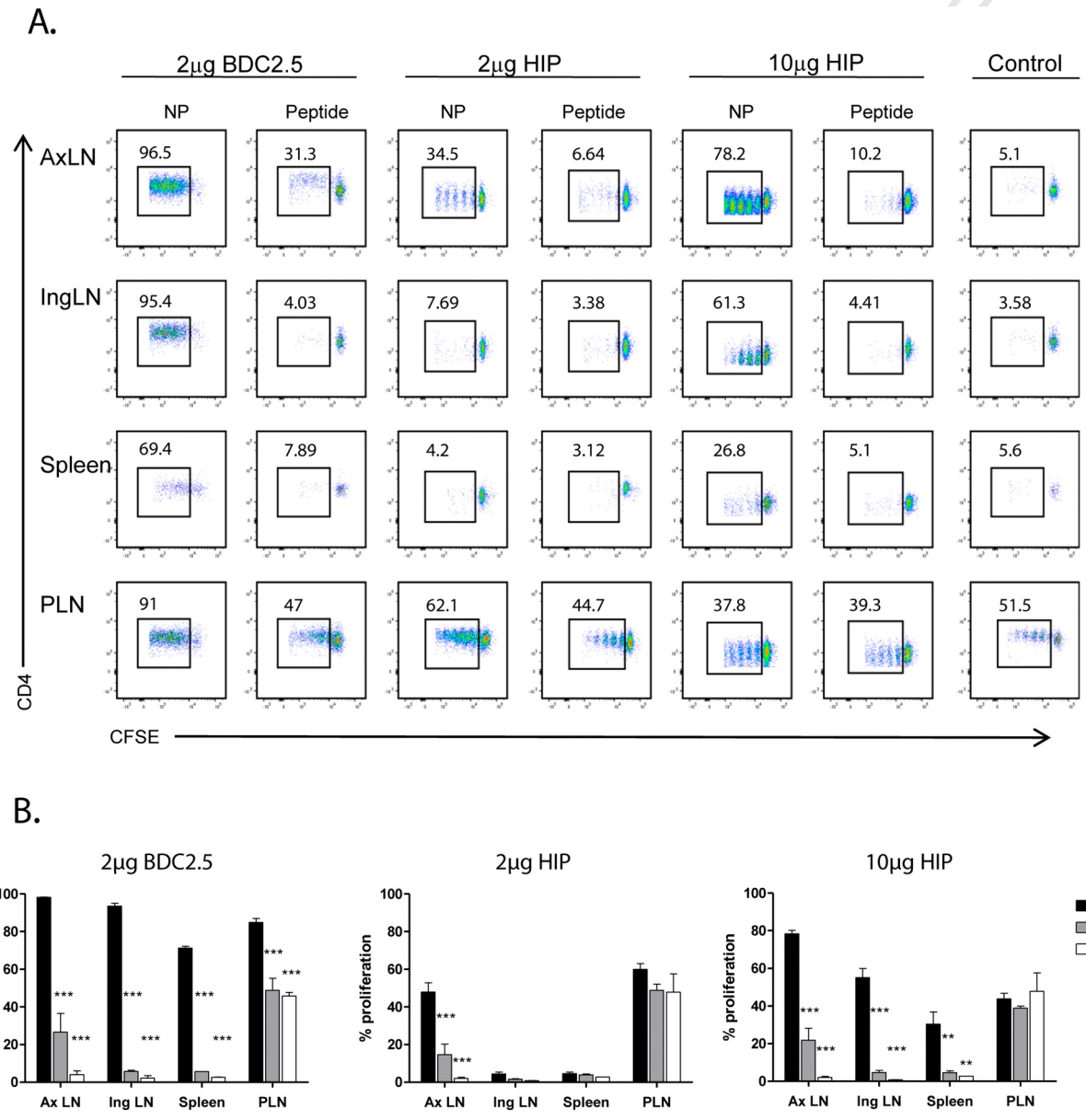


Figure 3. **Peptide-NP effects on in vivo T-cell proliferation are dependent on peptide affinity**. CFDA-labeled BDC2.5 CD4+ T-cells were transferred intravenously into NOD mice, followed by an ID injection of peptide or peptide-NP. LNs (axillary, inguinal and pancreatic) and spleen were harvested 72 h later and proliferation analyzed by flow cytometry. **(A)** Representative flow cytometric plots showing proliferative responses from left to right, 2 μg BDC2.5mimotope-NP, 2 μg BDC2.5mimotope peptide, 2 μg HIP-NP, 2 μg HIP peptide, 10 μg HIP-NP, 10 μg HIP peptide and no ID injection. **(B)** Left to right, summary of proliferation for high affinity BDC2.5mimotope and lower affinity 2 μg and 10 μg HIP epitope. Mean ± SEM of 3 mice per treatment is shown, representative of 3 experiments. Statistical analysis was done using one-way ANOVA with Bonferroni post-test comparing peptide-NP to peptide and control (**$P < 0.01$, ***$P < 0.001$).

BDC2.5mimotope-NP, though still significantly higher than HIP peptide alone. Endogenous proliferation in the pancreatic LN was not enhanced by 2 μg HIP-NP. No proliferation above control (no ID injection) was observed in the inguinal LN and spleen. However, when a higher dose of HIP-NP was administered (10 μg), widespread proliferation was observed in these NP-treated mice, with profiles resembling those witnessed with 2 μg BDC2.5mimotope NP. These results are consistent with lower amounts of peptide-NP being present in distant LN and in the case of a lower affinity peptide, may be limiting for T-cell proliferation at lower doses. Dissemination of peptide alone was much less efficient than its NP-formulated counterpart and therefore no presentation was witnessed in the distant LNs, at any of the doses of HIP peptide that were examined.

Peptide-NP conjugation: effects of peptide solubility

The influence of peptide solubility on peptide-NP behavior was also evaluated in vivo (Figure 4), by comparing the behavior of the highly water-soluble OTII peptide, recognized by OTII CD4+ T-cells, with the less soluble BDC2.5mimotope and HIP peptide counterparts. CTV-labeled cells were transferred into C57BL/6 mice, followed by OTII peptide or OTII-NP at 2 μg or 10 μg by ID injection, using 29G insulin needles. At a 2 μg OTII-NP dose, T-cell proliferation occurred in all the lymphoid organs, with greatest proliferation in the draining lymph nodes (brachial and axillary LN). Moreover, at the higher dose of 10 μg, OTII-NP induced significantly more T-cell proliferation than 2 μg OTII-NP in the inguinal LN ($^{**}P < 0.01$) and spleen ($^{***}P < 0.001$). In contrast to both BDC2.5mimotope and HIP peptide, proliferation of T-cells in response to the OTII peptide also reached almost 100%.

Peptide-NP can be successfully delivered via MicronJet600™ microneedles into murine skin

To test whether using MicronJet600™ MNs would enhance peptide-NP and free peptide delivery in vivo, experiments were performed in both NOD and C57BL/6 mice. Following intravenous transfer of BDC2.5 CD4+ T-cells into NOD mice (Figure 5), and OTII cells into C57BL/6 mice (Figure 6), the respective mice were injected with 2 μg BDC2.5mimotope-NP or 2 μg OTII peptide-NP or soluble peptide using MicronJet MNs. Lymphoid organs were harvested after 72 h and proliferation was analyzed. Figures 5 and 6 indicate successful peptide-NPs delivery using MNs, with high levels of proliferation in the skin-draining brachial and axillary LN, as well as the inguinal LN and spleen, thus confirming the presentation of the MN-delivered antigen to the responding T-cells. However, the use of MicronJet needles, in this context, did not enhance delivery of the BDC2.5mimotope peptide alone, nor alter the delivery of OTII peptide compared to conventional ID injection. Overall, proliferation following MN delivery was comparable to that observed with conventional ID injection.

Peptide-NP is transported to LN by migratory skin DCs

CCR7, a leukocyte chemotactic receptor, is expressed by mature DCs and plays a key role in DC homing to LNs, as well as their subsequent positioning within LN functional compartments. Loss of CCR7 impedes DC migration from non-lymphoid organs, such as the skin, into the draining LN.[25,27] With this in mind, CCR7-deficient mice were used to determine the role of DCs in distribution of OTII peptide and OTII peptide-NP, and to determine whether peptide transport is an active DC-mediated process. ID injection of OTII peptide and OTII-NP was therefore examined at two different concentrations (2 μg and 10 μg) in wild type C57BL/6 or CCR7KO C57BL/6 mice. A reduction in proliferation was observed in different LN of the CCR7KO mice following administration of the peptide-NP, with a significant reduction at the higher 10 μg OTII concentration in both the draining LN and spleen ($^{*}P < 0.05$) (Figure 7). Although the same trend was observed with 2 μg OTII-NP and peptide alone, the decrease was not statistically significant. This suggests that migratory DCs are important for peptide-NP transport from the skin to the draining LNs, particularly at high concentrations.

HIP-NP influences cellular phenotype in a concentration-dependent manner

To determine the impact of HIP-NP concentration on cell function, NOD mice were transferred with CFDA-labeled BDC2.5 CD4+ T-cells and then immediately treated with an ID injection of 0.4 μg, 2 μg, 6 μg or 10 μg HIP-NP or free HIP peptide. After 72 h, axillary draining LNs, the inguinal LN, spleen and pancreatic LN were harvested and examined and a concentration dependent HIP-NP proliferative response was revealed. Proliferation in the axillary LN, inguinal LN and spleen, was most notable at 10 μg. This was significantly higher than the proliferation observed in the HIP peptide-administered mice (Figure 8, *A*) and consistent with experiments that were conducted with a more limited dose range (Figure 3). Furthermore, the axillary LN T-cells expressed increased levels of activation markers CD44 and CTLA4 (Figure 8, *B*), which reached significance at lower concentrations compared with proliferation in the inguinal LN and spleen. Despite enhanced activation status, a significant decrease in cells expressing IFNγ was noted in the axillary LN of HIP-NP treated mice compared to peptide alone ($^{*}P < 0.05$). IL-10 expression was low under all conditions (Figure 8, *C*). Therefore, while T-cells displayed an increased activation and proliferation profile over a wide HIP-NP range, functionally the cells of the draining LN produced less IFNγ.

Discussion

The lipophilicity of 'naked' peptide autoantigens has been shown to influence localized delivery in human skin[28]; results in murine skin (Figures 2-6) provide further exemplification of this. The murine dermis is an aqueous region, consisting of 60.3% water,[29] and therefore the notable increase in T-cell proliferation in response to intradermal administration of the water-soluble OTII peptide (its cognate antigen) at lymphoid organs distant to the local environment (Figure 7) is likely to be facilitated by rapid diffusion in the local environment, uptake by DC in draining LNs and subsequent distribution in the lymphatic system. However more lipophilic auto-antigenic peptides such as BDC2.5mimotope and HIP, which are insoluble in aqueous

UNCORRECTED PROOF

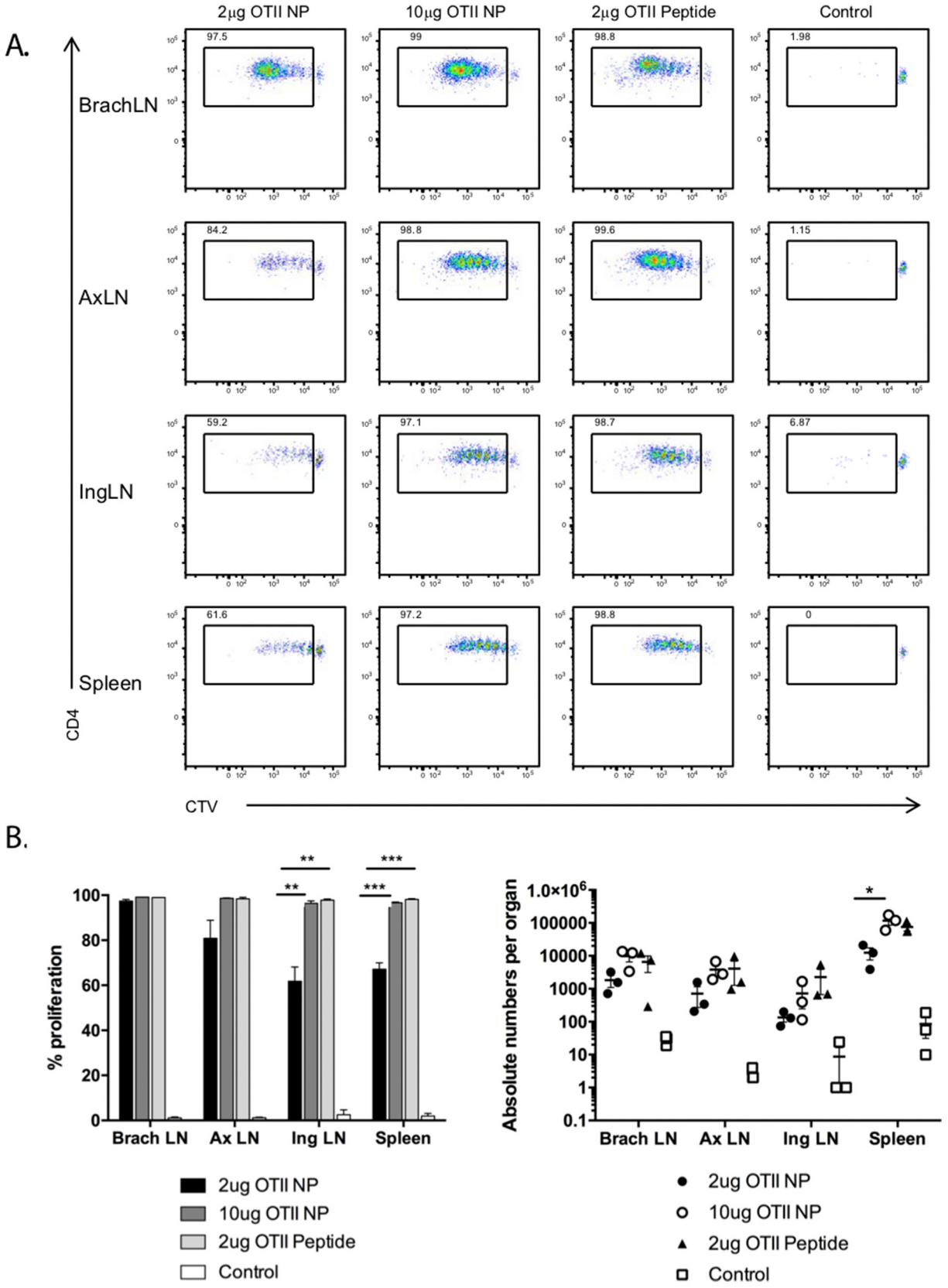
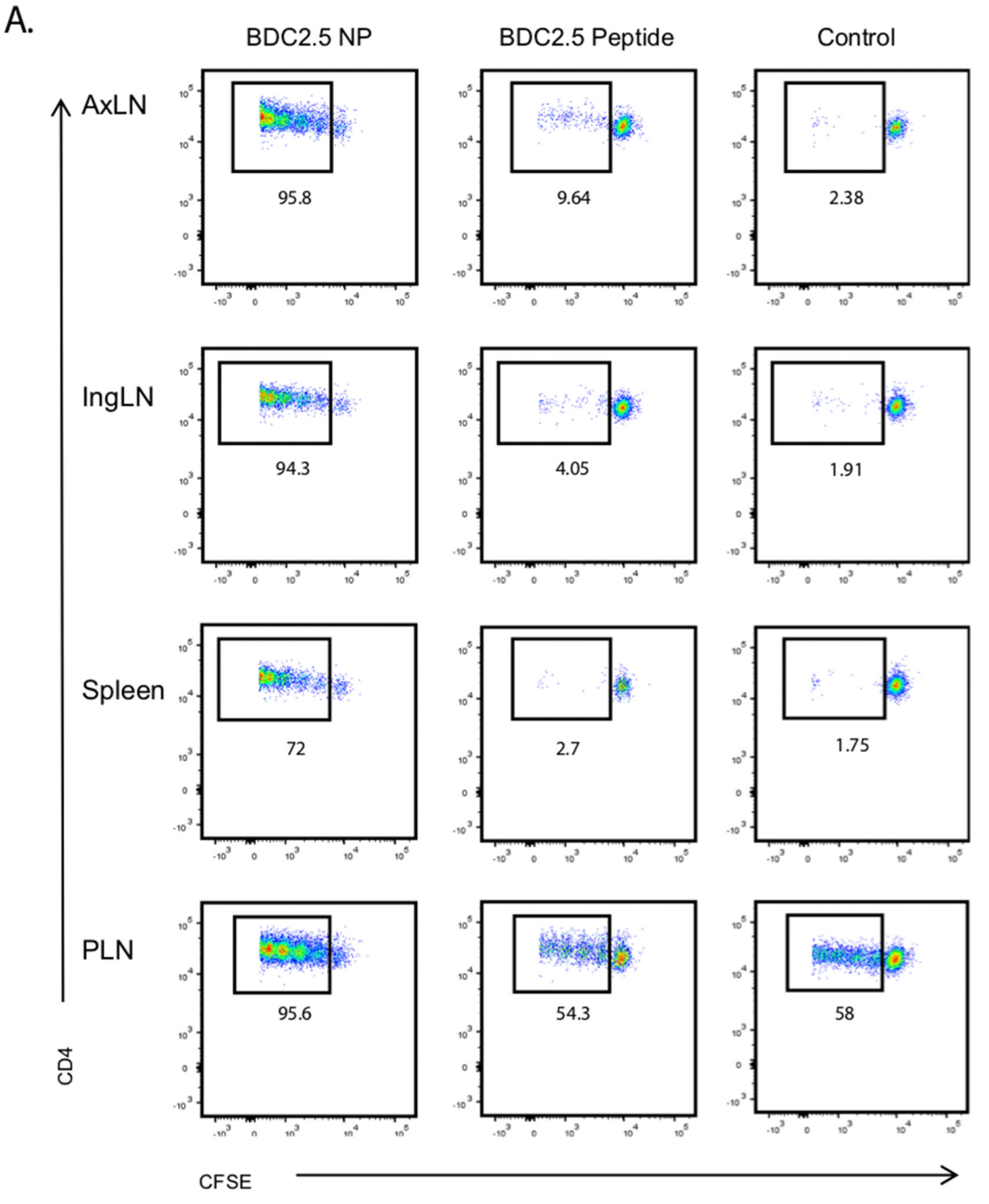


Figure 4. **Peptide-NP effects in vivo differ according to peptide solubility. (A)** Representative flow cytometric plots showing proliferative responses to (from left to right) 2 μg OTII-NP, 10 μg OTII-NP, 2 μg OTII peptide and controls in the brachial and axillary LNs (draining), distal inguinal lymph node and spleen. **(B)** Summary of proliferation for OTII-NP and peptide by % proliferation and absolute numbers. Data represent mean ± SEM (% proliferation) and each dot


A.
BDC2.5 NP
BDC2.5 Peptide
Control
AxLN
IngLN
Spleen
PLN
95.8
9.64
2.38
94.3
4.05
1.91
72
2.7
1.75
95.6
54.3
58
CD4
CFSE
B.
% proliferation
100
80
60
40
20
0
***
**
Ax LN
Ing LN
Spleen
PLN
BDC2.5 NP
BDC2.5 Peptide
Control

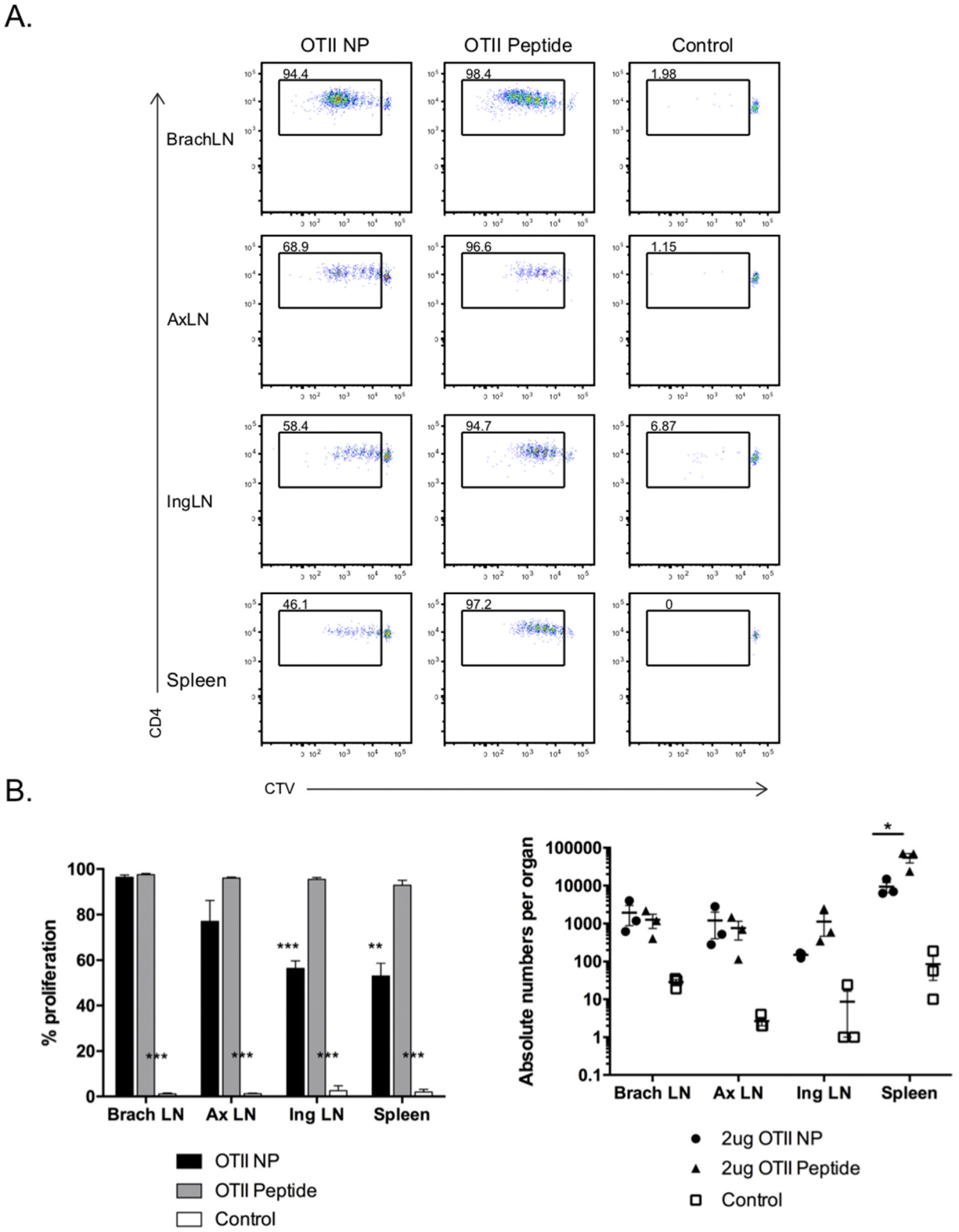


Figure 6. **MicronJet600 ™ delivery of OTII peptide-NP and peptide alone induce proliferation of transferred T-cells**. Mice received fluorescently-labeled cells intravenously, followed by an ID injection of peptide or peptide-NP using the short (600 μm) hollow MN device (MicronJet600TM). Lymph nodes were harvested 72 h later and proliferation was analyzed by flow cytometry. **(A)** Representative flow cytometric plots showing proliferative responses to 2 μg OTII-NP, 2 μg OTII peptide and controls in the brachial and axillary lymph nodes (draining), distal inguinal lymph node and spleen following MN delivery. **(B)** Summary of proliferation for OTII-NP and peptide. Mean ± SEM (% proliferation) is shown and each dot corresponds to a mouse (absolute numbers per organ). Data are representative of three experiments with n = 2-3 animals per group. Significant differences were identified using one-way ANOVA with Bonferroni post-test comparing peptide-NP to peptide and control (**$P < 0.01$ ***$P < 0.001$).

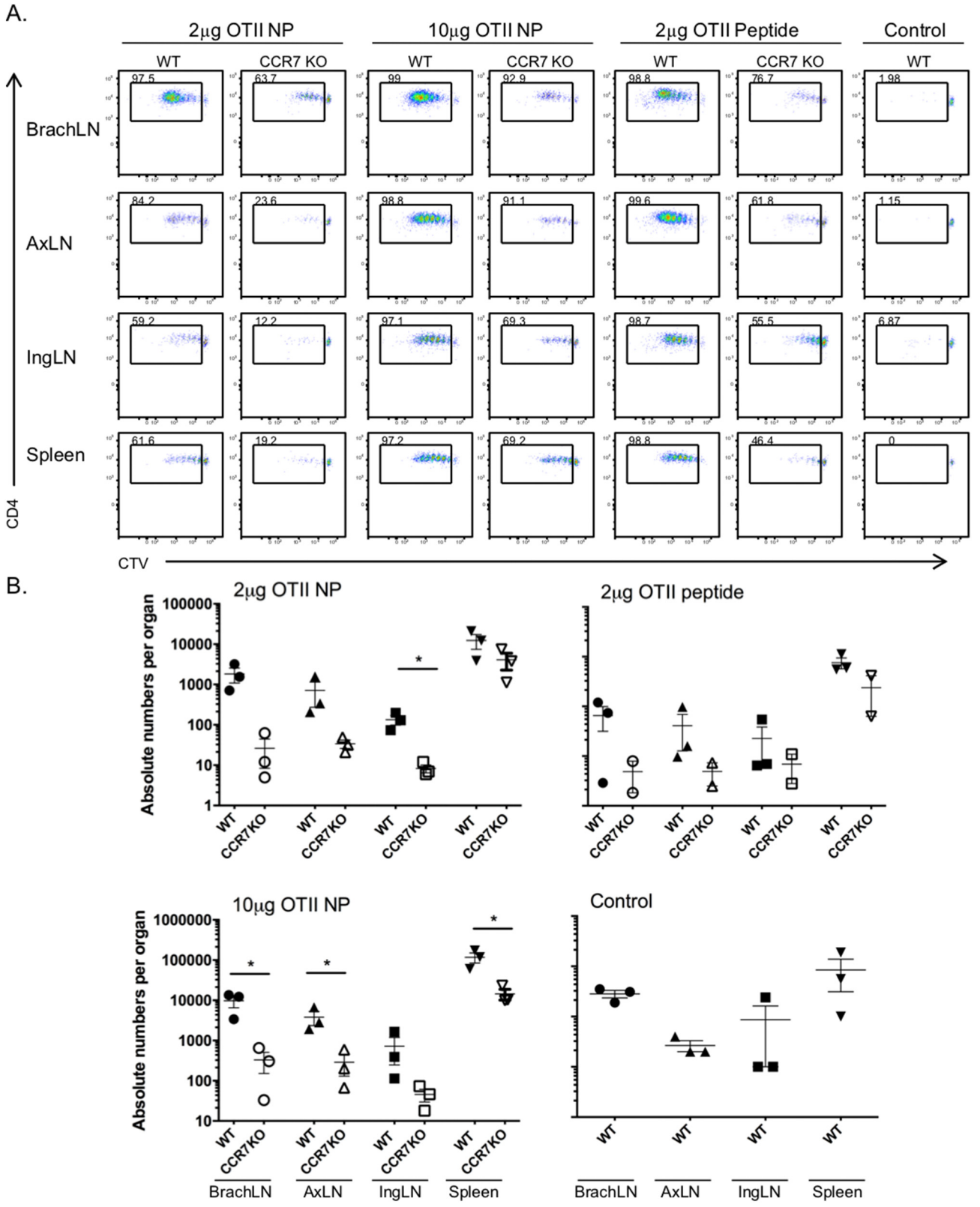


Figure 7. **Peptide-NP is taken up by dendritic cells and distributed to lymphoid organs.** WT and CCR7KO mice received CTV-labeled OTII T-cells intravenously, followed by an ID injection of peptide or peptide-NP using a 600 μm MicronJet600™ needle. LNs and spleen were harvested 72 h later and proliferation was analyzed by flow cytometry. **(A)** Representative flow cytometric plots showing proliferative responses (left to right) to 2 μg OTII-NP, 10 μg OTII-NP, 2 μg OTII peptide and controls in the brachial and axillary LN (draining), distal inguinal LN and spleen. **(B)** Absolute numbers of proliferating OTII CD4+ T-cells in response to OTII-NP and peptide. Each dot corresponds to a mouse and the mean (horizontal bar) is indicated. Data are representative of three

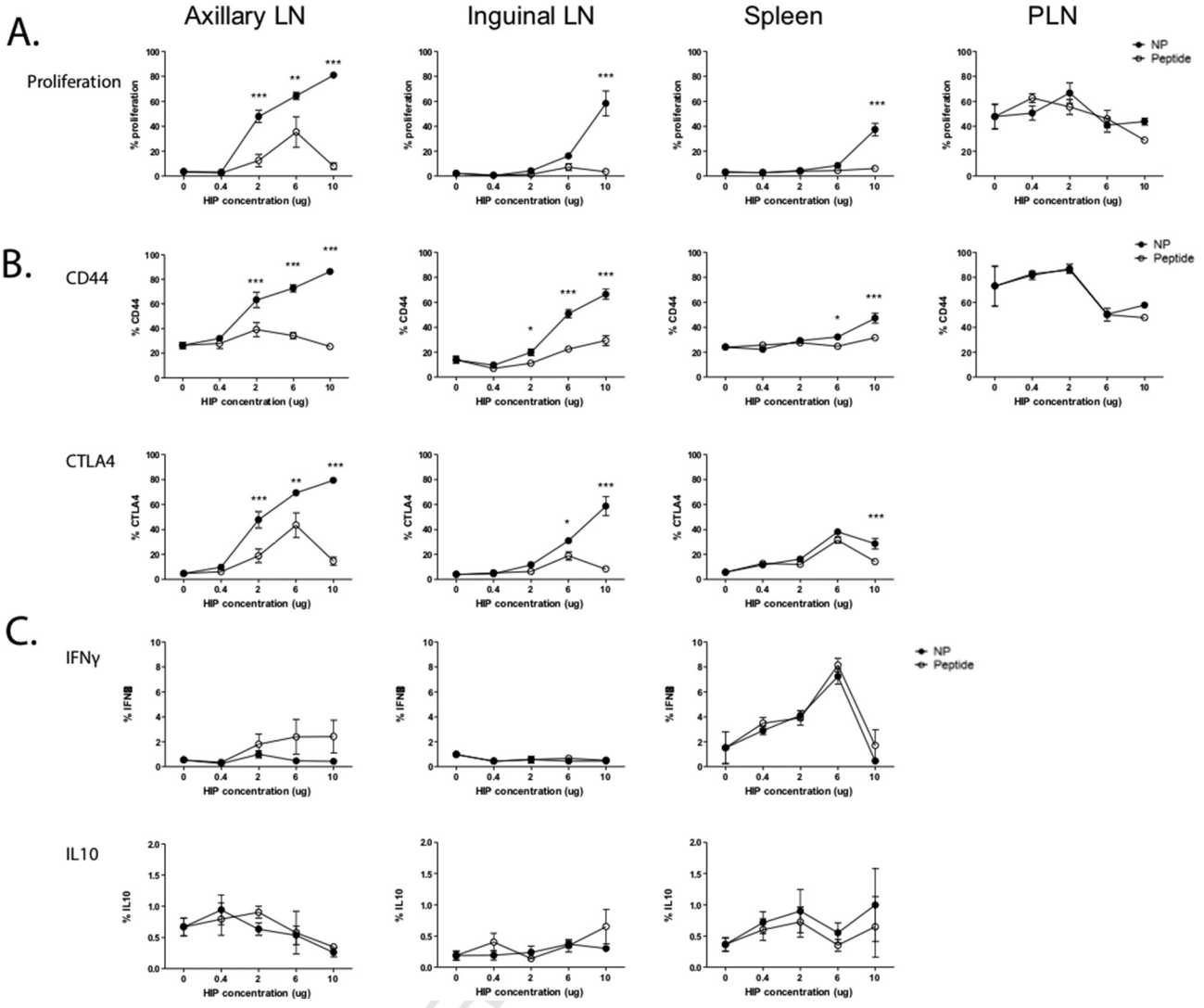


Figure 8. **HIP-NP has differential effects on the cellular phenotype dependent on concentration.** NOD mice received CFDA-labeled BDC2.5 CD4+ T-cells intravenously, followed immediately by an ID injection (29G insulin needle) of HIP-NP or HIP peptide at various concentrations. LNs were harvested 72 h later and CD4+ T-cells were analyzed by flow cytometry. **(A)** Proliferative response of cells to HIP-NP or peptide as determined by CFSE dilution. **(B)** BDC2.5 T-cell activation markers including CD44 and CTLA4 and **(C)** cytokine response including IFNγ (axillary LN; interaction = ns, NP vs peptide p = *0.027, HIP concentration = ns) and IL10. Statistical analysis was done using two-way ANOVA with Bonferroni post-test comparing peptide-NP and peptide at individual concentrations (*$P < 0.5$ **$P < 0.01$, ***$P < 0.001$). Mean ± SEM is shown; data are representative of 3 experiments ($n = 3$ per treatment).

media, such as water and PBS, are only able to stimulate response in the local environment i.e. in the draining lymph node (Figures 2-3). Enhancing the distribution of poorly water-soluble peptides to stimulate immune responses distant from their administration site may be desirable for a range of therapeutic approaches, including immunotherapy for conditions such as type 1 diabetes.

Gold NPs have recently garnered attention as drug delivery agents for several reasons, including their lack of toxicity,[31] chemical stability and extensive surface to volume ratio,[32,33] which enable conjugation of clinically significant doses of therapeutics. NPs have previously been used to deliver disease-relevant autoantigens in mouse models of EAE,[34–36] arthritis[37,38] and diabetes.[18,19,39] Therefore, in this study we have explored the potential of a gold NP formulation to enhance trafficking of lipophilic peptides from the antigen-presenting cell (APC) rich skin compartment to distant target sites, such as the pancreas and pancreatic LN. We have also investigated the importance of the mechanism of administration (microneedles versus ID injection), peptide affinity, peptide solubility and dosing on peptide-NP trafficking in vivo.

Peptide-NPs incorporating the relatively insoluble BDC2.5mimotope and HIP peptides facilitated enhanced proliferation at LNs distant to the site of intradermal injection, thus indicating a marked improvement in distribution, in vivo, compared to peptide alone. Enhanced proliferation of T-cells, in response to the NP-conjugated lipophilic peptides, was detectable in the draining LN, the non-draining LN, the spleen and the PLN, 48 h after intradermal administration. These kinetics are consistent with a minimum requirement of 24 h for T-cell

proliferation to occur after antigen encounter. Conversely, conjugation of the highly water-soluble OTII peptide to the NP formulation reduced proliferation in the LNs at a "like for like" dose (2 μg) and it was only at an increased dose (10 μg) that the NP formulation performed comparably to the 'naked' peptide. This may be explained by a reduction in the diffusive properties of the hydrophilic peptide upon conjugation to a gold NP and, as a corollary, indicates that the enhancement afforded by conjugation of the lipophilic peptides to the ultra-small gold NPs may not be mediated simply by an increase in the solubility and diffusive properties of the therapeutic within the tissue. However, while these results are indicative, the lipophilic and hydrophilic peptides used in this study are detected by two different T-cell clones in two different mouse strains. Future experiments examining a range of peptide solubilities in a single mouse strain are therefore needed to probe this hypothesis further. Further studies could also explore whether NP-conjugation enhances peptide stability in vivo, as this may also contribute to enhanced and prolonged T-cell proliferation.

DCs are abundant in the immunocompetent skin. Increased peptide uptake by DCs in the local environment is more likely to result in increased activation and translocation of these highly effective APCs from the skin to the draining LNs and subsequent presentation to their cognate T-cells. Studies conducted in the CCR7-deficient mouse model at high OTII-NP concentrations (Figure 7) were therefore used to probe the role of DCs in trafficking locally-delivered NP-conjugated lipophilic peptides to distant LNs. Data indicate that distribution to LNs was partly dependent on DCs, with those mice lacking the lymph node homing receptor, CCR7, displaying reduced proliferation in response to peptide-NP administration (Figure 7). Previous studies suggest that intradermally-delivered antigens conjugated to a NP formulation diffuse within the extracellular environment to the draining LN for presentation to resident DCs in a size-dependent manner.[5,42,43,45,46] Furthermore, it has been hypothesized that 'large' NPs, ranging from 33 nm[45] to 500 nm,[46] are internalized by DCs at the site of injection and are trafficked to local LNs for presentation, while 'small' NPs are not retained in LNs, thereby reducing the magnitude and quality of the ensuing T-cell response[45,47] and Foxp3 T-reg induction.[43,48] In contrast to this, we have shown that ultra-small OTII-NPs (2-6 nm) are, in part, taken up by DCs following ID injection and are subsequently transported to the local draining LN. Mice deficient in the LN homing receptor CCR7 demonstrated significantly less proliferation in the draining LN, particularly at the high concentration peptide-NP formulation. We therefore hypothesize that the enhancement in the distribution afforded by gold NP conjugation to poorly soluble peptides is, in part, due to enhanced trafficking from the site of injection by DCs, rather than simply by a change to the diffusive properties of the formulation. This finding is of particular interest, as it implies that peptide-NPs could be formulated with a second tolerogenic cargo that could be targeted and co-delivered to skin DCs (rather than LN resident DCs that may be responsible for presentation of 'naked' peptide that reaches the LN by diffusion), thus potentially enabling DC function to be modulated prior to migration to the draining LN.

Different affinities of the peptides to their corresponding antigen-specific T-cells resulted in observable differences in the in vivo response to the BDC2.5mimotope, HIP and OTII peptide-bound NP formulations. BDC2.5mimotope peptide, identified by screening a peptide library,[23] has a high affinity to BDC2.5 CD4+ T-cells whereas HIP, a relatively newly-discovered peptide epitope, has been proposed as the natural peptide for the highly diabetogenic BDC2.5 T-cells and thus, in common with many autoantigens, is relatively lower affinity.[22] This relationship was maintained following NP conjugation of the peptides, with HIP-NPs inducing less proliferation than BDC2.5mimotope-NPs at the same peptide dose, thus indicating that NP conjugation to the peptide does not have a detrimental effect on the relative potencies of these auto-antigens.

Previous studies using NPs formulated with an islet autoantigen provide evidence that enhanced expansion of regulatory T-cells in lymphoid organs may translate to a tolerogenic response in diabetes mouse models.[18,19] This was exemplified by an expansion in T regulatory cells and suppression of diabetes development; however neither study delivered antigen by the intradermal route.[18,19] In both of these studies the authors reasoned that NPs would also benefit from a second tolerance-inducing cargo. Indeed, sub-cutaneous delivery of antigen-specific NP formulations, intended to induce tolerance in vivo, has typically used additional anti-inflammatory mediators, such as IL10,[42] rapamycin[34] or TGFβ.[43] HIP-NP studies were therefore extended to explore whether intradermal delivery and enhanced distribution of the peptide to distant LNs could bring about a phenotypic change that is indicative of tolerance in type 1 diabetes i.e. a reduction in IFNγ, a pro-inflammatory cytokine whose levels correlate with disease progression and which is known to enhance the development of type 1 diabetes in the NOD mouse model.[40,41] Down-regulation of this pro-inflammatory mediator IFNγ, three days after administration of HIP-NPs (Figure 7), therefore encourages further investigation of HIP-NP as a therapeutic candidate, potentially a pro-tolerogenic addition to the NP formulation to further enhance regulation.

In this study, NPs were administered via an ID injection using both traditional hypodermic needles and hollow MNs (MicronJet600™). In the mouse model, both methods were able to deliver both peptide and peptide NP formulations into the skin and facilitated comparable in vivo responses. While there are well-recognized differences in murine and human skin, here, both methods of delivery proved equal in their ability to deliver peptide and peptide-NP. Both methods are easily translatable to humans, and peptide and peptide-NP are presented in LNs distant to the site of injection.[9]

In conclusion, this study illustrates the potential value of the intradermal delivery of ultra-small gold NPs for enhanced delivery of lipophilic peptide autoantigens to lymphoid organs and the importance of peptide dose, affinity and solubility on distribution to, and T-cell expansion at, these body sites. Peptide-NP formulations therefore potentially provide a valuable means of targeting poorly soluble peptide epitopes to internal directly inaccessible LNs, such as the pancreatic LN, which may be of particular value in type 1 diabetes tolerisation strategies. Future

UNCORRECTED PROOF

studies will investigate the clinical utility of this drug delivery system in immunotherapy.

Uncited references

30, 44

Acknowledgments

We thank Drs Kathryn Haskins and Thomas Delong for early information regarding the HIP peptide prior to publication.

References

1.. Anderson MS, Bluestone JA. The NOD mouse: a model of immune dysregulation. *Annu Rev Immunol* 2005;**23**:447-85.
2.. Guilliams M, Henri S, Tamoutounour S, Ardouin L, Schwartz-Cornil I, Dalod M, et al. From skin dendritic cells to a simplified classification of human and mouse dendritic cell subsets. *Eur J Immunol* 2010;**40**:2089-94.
3.. Henri S, Guilliams M, Poulin LF, Tamoutounour S, Ardouin L, Dalod M, et al. Disentangling the complexity of the skin dendritic cell network. *Immunol Cell Biol* 2010;**88**:366-75.
4.. Romani N, Flacher V, Tripp CH, Sparber F, Ebner S, Stoitzner P. Targeting skin dendritic cells to improve intradermal vaccination. *Curr Top Microbiol Immunol* 2012;**351**:113-38.
5.. Romani N, Thurnher M, Idoyaga J, Steinman RM, Flacher V. Targeting of antigens to skin dendritic cells: possibilities to enhance vaccine efficacy. *Immunol Cell Biol* 2010;**88**:424-30.
6.. Gupta J, Park SS, Bondy B, Felner EI, Prausnitz MR. Infusion pressure and pain during microneedle injection into skin of human subjects. *Biomaterials* 2011;**32**:6823-31.
7.. Coulman S, Allender C, Birchall J. Microneedles and other physical methods for overcoming the stratum corneum barrier for cutaneous gene therapy. *Crit Rev Ther Drug Carrier Syst* 2006;**23**:205-58.
8.. Kochba E, Levin Y, Raz I, Cahn A. Improved insulin pharmacokinetics using a novel microneedle device for intradermal delivery in patients with type 2 diabetes. *Diabetes Technol Ther* 2016;**18**:525-31.
9.. Levin Y, Kochba E, Kenney R. Clinical evaluation of a novel microneedle device for intradermal delivery of an influenza vaccine: are all delivery methods the same? *Vaccine* 2014;**32**:4249-52.
10.. Levin Y, Kochba E, Shukarev G, Rusch S, Herrera-Taracena G, van Damme P. A phase 1, open-label, randomized study to compare the immunogenicity and safety of different administration routes and doses of virosomal influenza vaccine in elderly. *Vaccine* 2016;**34**:5262-72.
11.. Beals CR, Railkar RA, Schaeffer AK, Levin Y, Kochba E, Meyer BK, et al. Immune response and reactogenicity of intradermal administration versus subcutaneous administration of varicella-zoster virus vaccine: an exploratory, randomised, partly blinded trial. *Lancet Infect Dis* 2016;**16**:915-22.
12.. Troy SB, Kouiavskaia D, Siik J, Kochba E, Beydoun H, Mirochnitchenko O, et al. Comparison of the immunogenicity of various booster doses of inactivated polio vaccine delivered intradermally versus intramuscularly to HIV-infected adults. *J Infect Dis* 2015;**211**:1969-76.
13.. Anand A, Zaman K, Estivariz CF, Yunus M, Gary HE, Weldon WC, et al. Early priming with inactivated poliovirus vaccine (IPV) and intradermal fractional dose IPV administered by a microneedle device: a randomized controlled trial. *Vaccine* 2015;**33**:6816-22.
14.. Levin Y, Kochba E, Hung I, Kenney R. Intradermal vaccination using the novel microneedle device MicronJet600: past, present, and future. *Hum Vaccin Immunother* 2015;**11**:991-7.
15.. Fadeel B, Garcia-Bennett AE. Better safe than sorry: understanding the toxicological properties of inorganic nanoparticles manufactured for biomedical applications. *Adv Drug Deliv Rev* 2010;**62**:362-74.
16.. de Araujo RFJ, de Araujo AA, Pessoa JB, Freire Neto FP, da Silva GR, Leitao Oliveira AL, et al. Anti-inflammatory, analgesic and anti-tumor properties of gold nanoparticles. *Pharmacol Rep* 2017;**69**:119-29.
17.. Compostella F, Pitirollo O, Silvestri A, Polito L. Glyco-gold nanoparticles: synthesis and applications. *Beilstein J Org Chem* 2017;**13**:1008-21.
18.. A. Yeste, M.C. Takenaka, I.D. Mascanfroni, M. Nadeau, J.E. Kenison, B. Patel, A.M. Tukpah, J.A. Babon, M. DeNicola, S.C. Kent, D. Pozo, F.J. Quintana, Tolerogenic nanoparticles inhibit T-cell-mediated autoimmunity through SOCS2, Sci Signal, 9 (2016) ra61.
19.. Clemente-Casares X, Blanco J, Ambalavanan P, Yamanouchi J, Singha S, Fandos C, et al. Expanding antigen-specific regulatory networks to treat autoimmunity. *Nature* 2016;**530**:434-40.
20.. Dul M, Nikolic T, Stefanidou M, McAteer MA, Williams P, Mous J, et al. Conjugation of a peptide autoantigen to gold nanoparticles for intradermally administered antigen specific immunotherapy. *Int J Pharm* 2019;**562**:303-12.
21.. Katz JD, Wang B, Haskins K, Benoist C, Mathis D. Following a diabetogenic T-cell from genesis through pathogenesis. *Cell* 1993;**74**:1089-100.
22.. Delong T, Wiles TA, Baker RL, Bradley B, Barbour G, Reisdorph R, et al. Pathogenic CD4 T-cells in type 1 diabetes recognize epitopes formed by peptide fusion. *Science* 2016;**351**:711-4.
23.. V. Judkowski, C. Pinilla, K. Schroder, L. Tucker, N. Sarvetnick, D.B. Wilson, Identification of MHC class II-restricted peptide ligands, including a glutamic acid decarboxylase 65 sequence, that stimulate diabetogenic T-cells from transgenic BDC2.5 nonobese diabetic mice, J Immunol, 166 (2001) 908–917.
24.. Barnden MJ, Allison J, Heath WR, Carbone FR. Defective TCR expression in transgenic mice constructed using cDNA-based [agr]- and [bgr]-chain genes under the control of heterologous regulatory elements. *Immunol Cell Biol* 1998;**76**:34-40.
25.. Forster R, Schubel A, Breitfeld D, Kremmer E, Renner-Muller I, Wolf E, et al. CCR7 coordinates the primary immune response by establishing functional microenvironments in secondary lymphoid organs. *Cell* 1999;**99**:23-33.
26.. Dul M, Stefanidou M, Porta P, Serve J, O'Mahony C, Malissen B, et al. Hydrodynamic gene delivery in human skin using a hollow microneedle device. *J Control Release* 2017;**265**:120-31.
27.. Förster R, Davalos-Misslitz AC, Rot A. CCR7 and its ligands: balancing immunity and tolerance. *Nat Rev Immunol* 2008;**8**:362-71.
28.. Zhao X, Coulman SA, Hanna SJ, Wong FS, Dayan CM, Birchall JC. Formulation of hydrophobic peptides for skin delivery via coated microneedles. *J Control Release* 2017;**265**:2-13.
29.. Suntzeff V, Carruthers C. The water content in the epidermis of mice undergoing carcinogenesis by methylcholanthrene. *Cancer Res* 1946;**6**:574-7.
30.. Steinman RM, Hawiger D, Nussenzweig MC. Tolerogenic dendritic cells. *Annu Rev Immunol* 2003;**21**:685-711.
31.. Merchant B. Gold, the noble metal and the paradoxes of its toxicology. *Biologicals* 1998;**26**:49-59.
32.. Farooq MU, Novosad V, Rozhkova EA, Wali H, Ali A, Fateh AA, et al. Gold nanoparticles-enabled efficient dual delivery of anticancer therapeutics to HeLa cells. *Sci Rep* 2018;**8**:2907.
33.. Dreaden EC, Austin LA, Mackey MA, El-Sayed MA. Size matters: gold nanoparticles in targeted cancer drug delivery. *Ther Deliv* 2012;**3**(4):457-78.
34.. Maldonado RA, LaMothe RA, Ferrari JD, Zhang AH, Rossi RJ, Kolte PN, et al. Polymeric synthetic nanoparticles for the induction of antigen-specific immunological tolerance. *Proc Natl Acad Sci U S A* 2015;**112**:E156-E165.
35.. Yeste A, Nadeau M, Burns EJ, Weiner HL, Quintana FJ. Nanoparticle-mediated codelivery of myelin antigen and a tolerogenic small molecule

UNCORRECTED PROOF

Q21	Uncited references: This section comprises references that occur in the reference list but not in the body of the text. Please position each reference in the text or, alternatively, delete it. Thank you. Please check this box if you have no corrections to make to the PDF file. ☐

Thank you for your assistance.